Damage Evolution of Underground Structural Reinforced Concrete Small-Scale Static-Loading Experiments

Ahmed Mohammed Youssef Mohammed, Mohammad Reza Okhovat, and Koichi Maekawa

Abstract—Small-scale RC models of both piles and tunnel ducts were produced as mockups of reality and loaded under soil confinement conditionsto investigate the damage evolution of structural RC interacting with soil. Experimental verifications usinga 3D nonlinear FE analysis program called COM3D, which was developed at the University of Tokyo, are introduced. This analysis has been used in practice for seismic performance assessment of underground ducts and in-ground LNG storage tanks in consideration of soil-structure interactionunder static and dynamic loading. Varying modes of failure of RCpilessubjected to different magnitudes of soil confinement were successfully reproduced in the proposed small-scale experiments and numerically simulated as well. Analytical simulation was applied to RC tunnel mockups under a wide variety of depth and soil confinement conditions, and reasonable matching was confirmed.

Keywords—Soil-Structure Interaction, RC pile, RC Tunnel

I. INTRODUCTION

THE past major earthquakes (e.g. Niigata 1964, Alaska 1964, Hyogoken-Nanbu 1995, and Haiti 2010) have caused serious damage to on-ground and underground RC structures [1 and 2]. Detailed investigation of these instances of remarkable damage has led to further understanding of failure modes and the ultimate limit state, shedding light on aspects such as land sliding, soil liquefaction, soil-structure interaction and the required ductility of RC structural elements. Series of variant scale experiments under both static and dynamic loading have been carried out to gain a better understanding of the damage evolution of both RC and soils[3 and 4].

Earthquakes cannot be prevented, but their impacts can be managed to a large degree so that loss to life and property can be minimized. The authors seek highly inelastic behavioral simulation for risk assessment and seismic strengthening of existing infrastructure in service.

Ahmed Mohammed Youssef Mohammed is a Post-Doctoral Researcher, Department of Civil Engineering, The University of Tokyo, Japan(phone: +81-3-5841-7498; fax: +81-3-5841-6010; e-mail: mohammed@concrete.t.u-tokyo.ac.jp).

Mohammad Reza Okhovat holds a PhD degree from Department of Civil Engineering, The University of Tokyo and currently works for Damwatch Services Ltd., Wellington, New Zealand(Phone: +64-4-381-1344; Fax: +64-4-381-1301; E-mail: mohammad.okhovat@damwatch.co.nz)

Koichi MAEKAWAis Professor, Department of Civil Engineering, The University of Tokyo, Japan(phone: +81-3-5841-7498; fax: +81-3-5841-6010;e-mail: maekawa@concrete.t.u-tokyo.ac.jp).

To this end, experimental verification is understood to be indispensable for realizing performance-based design and maintenance to better cope with the hazards of future earthquakes. From this point of view, the authors provide a codified computational simulation method whose capability may be examined using small-scale RC piles and box type tunnel ducts. The pile mockups used were 5cm in diameter. Since the shear failure of RC members exhibits a size effect, it has been thought that shear failure cannot be reproduced using very small-scale alternatives, unlike the flexural mode of failure. In order to cancel this effect, the shear transfer of crack surfaces was intentionally reduced by using coarse-aggregate free composites with specialized deformed bars of small diameters not greater than 4 mm. Using this approach, realistic shear failure of RC piles was successfullyreplicated in the proposed experiments. Small-scale RCbox tunnel sectionsburied in soil were also tested with an artificially produced overlay. The ultimate limit states of RC box culverts and RC-soil systems were compared through both experiments and nonlinear analyses. The damage states were investigated by thesystematically verified finite element program called COM3D [5, 6, 7, and 8].

II. NONLINEAR CONSTITUTIVEMODELS

A. RC Constitutive model

A reinforced concrete material model was constructed by combining the constitutive laws for cracked concrete and those for reinforcement. The fixed multi-directional smeared crack constitutive equations [5]wereused as summarized in Fig 1. The crack spacing and diameters of reinforcing bars are implicitly taken into account in smeared and joint interface elements no matter how large they are.The constitutive equations of structural concrete satisfy uniqueness for compression, tension and shear transfer along crack planes. The bond between concrete and reinforcing bars is taken into account in the form of the tension stiffening model, and the space-averaged stress-strain relation of reinforcement is assumed to represent the localized plasticity of steel around concrete cracks. The hysteresis rule of reinforcement is formulated based upon Kato's model [9] for a bare bar under reversed cyclic loads. This RC in-plane constitutive modeling has been verified by member-based and structural-oriented experiments. Herein, the authors skip the details of the RC material modeling by referring to Maekawa et al. [5].
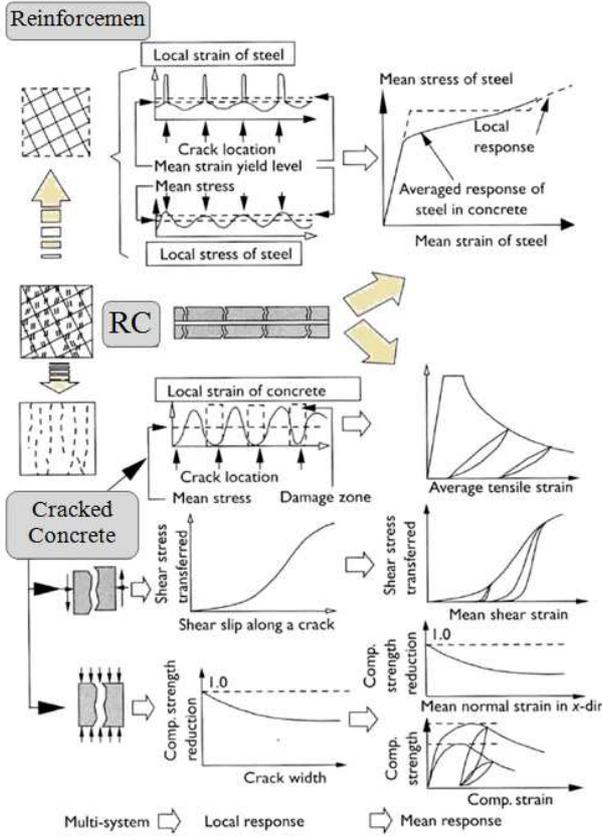
Fig. 1 RC constitutive laws [5]

B. Soil Constitutive Model

A nonlinear path-dependent constitutive model of soil is essential to simulate the entire RC-soil system. Here, the multi-yield surface plasticity concept [4, 5, and 10] is applied to formulate the shear stress-shear strain relation of the soil following Masing's rule [11].

The basic idea of this integral scheme is actualized to sum up component stresses that may represent microscopic events. First, the total stress applied on soil particle assembly, denoted by σ_{ij}, can be decomposed into the deviatoric shear stresses (s_{ij}) and the mean confining stress (p) as,

$$\sigma_{ij} = s_{ij} + p\delta_{ij} \qquad (1)$$

where δ_{ij} is Kronecker's delta symbol

Soil is idealized as an assembly of finite numbers of elasto-perfectly plastic components, which are conceptually connected in parallel as shown in Fig 2. As each component is given different yield strengths of plasticity, all components subsequently begin to yield at different total shear strains, which results in a gradual increase of entire nonlinearity. The nonlinear behavior appears naturally as a combined response of all components. Hence, the total shear stress carried by soil particles is expressed with regard to an integral of each component stress as,

$$s_{ij} = \sum_{m=1}^{n} s_{ij}^{m}(\varepsilon_{kl}, \varepsilon_{pkl}^{m}, G_{o}^{m}, F^{m})$$

$$ds_{ij}^{m} = 2G_{o}^{m} de_{eij}^{m} = 2G_{o}^{m}(de_{ij} - de_{pij}^{m})$$

$$de_{pij}^{m} = \frac{s_{ij}^{m}}{2F^{m}} df, \qquad (2)$$

$$df = \frac{s_{kl}^{m} de_{kl}}{F^{m}} = \frac{s_{kl}^{m} d\varepsilon_{kl}}{F^{m}}$$

Where ε_{kl} and ε_{pkl} are the total and plastic strain tensors, respectively, of the (k,l) component, G_{o}^{m} and F^{m} are the initial shear stiffness and the yield strength, respectively, of the m-th component, and (e_{ij}, e_{pij}^{m}, e_{eij}^{m}) are the deviatoric tensors of total strain, and those of plastic and elastic strains of the m-th component, respectively. These component parameters can be uniquely decided from the shear stress strain relation of soil under the referential constant confinement [6].
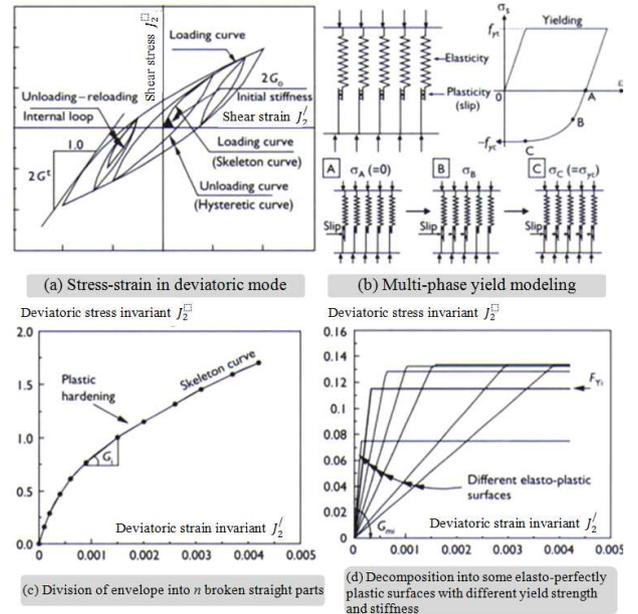

Fig. 2 Constitutive modeling for soil [5]

In general, the volumetric components may fluctuate and affect the shear strength of the soil skeleton. In reality, the shear strength of soil may decay when increasing pore water pressure leads to reduced confining stress of the soil particle skeleton. The multi-yield surface plastic envelope may inflate or contract according to the confinement stress as shown in Fig 3. It can be formulated by summing up the linear relation of the shear strength and the confinement stress as,

$$F^{m} = \chi F_{ini}^{m}$$

$$\chi = \frac{(c - I_{1}' \tan \phi)}{S_{u}} \qquad (3)$$

$$I_{1}' = \frac{(\sigma_{1}' + \sigma_{2}' + \sigma_{3}')}{3}$$

where S_{u} is the specific shear strength corresponding to a certain confinement (98kN), F_{ini}^{m} is the specified yield strength

of the m-th component corresponding to the specific S_u, χ is the confinement index, and (c, ϕ) are the cohesive stress and the friction angle, respectively.

For simulation of the pore water pressure and related softening of soil stiffness in shear, the volumetric nonlinearity of the soil skeleton has to be taken into account. The authors simply divided the dilatancy into two components according to the microscopic events. One component is the consolidation (negative dilation) as unrecoverable plasticity denoted by ε_{vc}. The other is the positive dilatancy associated with alternate shear stress due to the overriding of soil particles, which is denoted by ε_{vd} as,

$$p = 3K_0(\varepsilon_0 - \varepsilon_v), \quad \varepsilon_v = \varepsilon_{vc} + \varepsilon_{vd} \quad (4)$$

where K_0 is the initial volumetric bulk stiffness of soil particles assembly and can be calculated by assuming the initial elastic Poisson's ratio denoted by ν (=0.2) as,

$$K_0 = \frac{2(1+\nu)}{3(1-2\nu)}G_0 \quad (5)$$

The volume reduction of pores among soil particles will cause increasing pore pressure under undrained states, which may lead to liquefaction. According to experiments on sandy soils, we have,

$$\varepsilon_{vc} = \varepsilon_{v,\lim}\left\{1 - \exp\left(-2(J_{2p} + J_{2p,ini})\right)\right\} - \varepsilon_{vc,ini} \quad (6)$$

$$J_{2p} = \int dJ_{2p}, \quad dJ_{2p} \equiv \frac{1}{2}s_{kl} \cdot d\varepsilon_{kl} \quad (7)$$

where J_{2p} represents the accumulated shear strain invariant of the soil skeleton [6 and 13], and $\varepsilon_{v,lim}$ is the intrinsic volumetric compacting strain corresponding to the minimum void ratio as,

$$\varepsilon_{vc,ini} = \varepsilon_{v,\lim}\left\{1 - \exp(-2J_{2p,ini})\right\}$$
$$\varepsilon_{v,\lim} = 0.1\left(\log_{10} I_1'^{0.6} + 1.0\right) \quad (8)$$

The relative density of soil denoted by D_r is associated with the following relation, which can be used to inversely decide $J_{2p,ini}$, which is a constant corresponding to the initial compactness of soil particles:

$$D_r(\%) = \frac{\varepsilon_{vc,ini}}{\varepsilon_{v,\lim}} = \left\{1 - \exp(-2J_{2p,ini})\right\} \quad (9)$$

The shear provoked dilation, which is path-independent and defined by the updated shear strain intensity J_{2s}, is empirically formulated as,

$$\varepsilon_{vd} = \eta\frac{(aJ_{2s})^2}{1 + (aJ_{2s})^2}$$
$$J_{2s} = \sqrt{\frac{1}{2}e_{ij}e_{ij}}, \quad a = 25.0 \quad (10)$$
$$\eta = \frac{0.015(\varepsilon_{vc} + \varepsilon_{v,ini})}{\varepsilon_{v,\lim}}$$

The multi-yield surface plasticity model has two main advantages. First, it can easily simulate the shear cyclic responses by means of the simplified algorithm with rather few material constants. Second, the path-dependency of soil can be represented only by the plastic strains (e_{mpij}) of all constituent components. As the multi-component scheme has similarities with the contact density model of crack shear transfer [14] and the multi-directional crack modeling of reinforced concrete [5], higher stability of computing soil-RC structural interaction is made possible.

The multi-yield surface plasticity model has been used to simulate the static and seismic behaviors of nonlinear soil-structure systems [14 and 15]. Regarding the liquefiable soil-RC interaction, the applicability of the models used in this paper was examined and verified by Maki et al. [6].
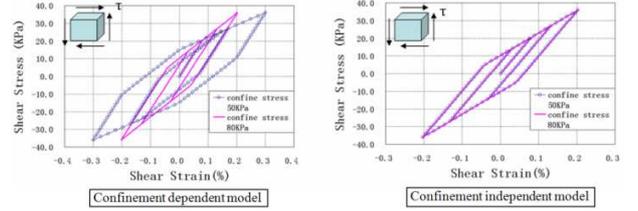

Fig. 3 Confinement dependent and independent models for soil [8]

III. RC PILE BENDING TEST

The experiment on miniature RC piles was carried out to show the positive and negative effects of soil confinement on RC pile damage evolution and also to examine the capability of simulation. Three small-scale RC pile specimens 5 cm in diameter and 60 cm in length were constructed with gravel-free mortar and four D4 deformed steel bars were installed into each pile (RFT ratio = 2.56%) as shown in Fig 4. In this mockup model, steel bars were hooked at both ends to avoid anchorage failure in the tension side. The mortar mix proportions used for the small-scale RC piles are listed in Table I. The specimens were cured in wet conditions for about 28 days and then loading was applied. The model concrete and steel bar properties are listed in Table II.
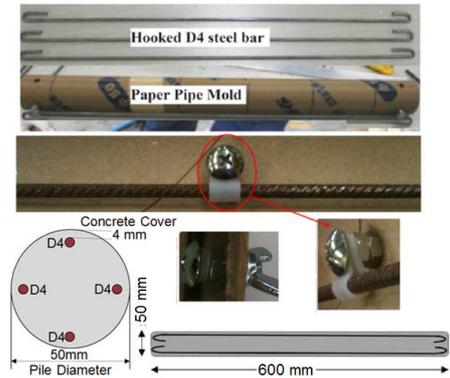

Fig. 4 RC pile cross section details

A. Experimental Setup of RC Pile Bending Test

Three RC piles were tested for bending subjected to three

TABLE I
MORTAR COMPONENTS

	W/C %	Sand %	Water (gr/lit)	Cement (gr/lit)	Sand (gr/lit)	(SP) (gr/lit)
RC Pile	40.0	100.0	324.9	812.3	1020.4	2.4
RC Tunnel	47.8	100.0	276.6	579.3	1000.0	0.0

TABLE II
MATERIAL PROPERTIES USED IN ANALYSIS OF RCPILE

Soil		Reinforced Concrete	
Poisson ratio	0.20	Compressive	55 MPa
Dry SG	1.6 kN/m³	Unit weight	25 kN/m³
Friction angle	35 °	Tensile strength	2.0 MPa
Relative density	40 %	Steel yYoung's modulus	2.1 x105 MPa
D50	0.2 mm	Steel yield stress	350 MPa

different levels of soil confinement (Low, Medium, and High), as shown in Table III. A rigid soil box (46.4cm x 70.0cm x 80cm) was fixed under the universal testing machine (UTM) and filled with Hamaoka sand to a depth of 10 cm. Each RC pile was hanged in a horizontal position from two stiff vertical hangers. Every hanger was connected by a set of hydraulic jack (20-tonf capacity) and load cell born on a rigid steel box beam, hydraulic jacks, and manually controlled pump, as illustrated in Fig 5. After that, the Hamaoka sand (Table IV) was poured with tamping up to a total soil depth of 60 cm and a set of two steel plates connected by a strong I-beam were placed on the soil top surface as shown in Fig 5.

TABLE III
EXPERIMENTAL VARIABLES

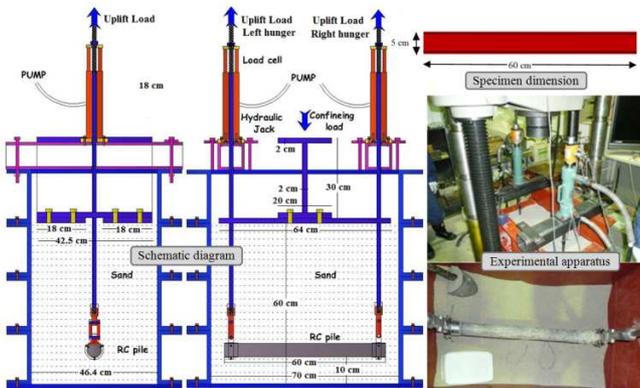| Cases	L.C	M.C	H.C
Confinement stress Kgf/cm2	0.3	0.6	1.2

Fig. 5 RC pile bending test under soil confinement

TABLE IV
SAND PROPERTIES USED IN THE EXPERIMENT

Specific gravity	2.687
Maximum unit weight	1.719 (N/mm3)
Minimum unit weight	1.429 (N/mm3)
Maximum void ratio	0.881
Minimum void ratio	0.564
D50	0.22 (mm)

After setting up all the experiment apparatus, two loading steps were carried out. First, while the top end nuts of the two hangers were released, the UTM's head was moved slowly

downward to bear on the I-beam's upper flange up to a certain load (confining load level, 10KN, 20KN, and 40KN). The vertical load was kept constant and uniformly distributed on the soil's top surface through two rectangular plates (64cm x 18cm x 2.2cm) bolted with and I-beam lower flange, as shown in Fig5. Second, after setting a certain level of confinement; the top end nuts of the hangers were manually tied and the two hangers were lifted. The load and displacement of every hanger were measured using load cells and displacement transducers.

B. Analytical Model of RC Pile Bending Test

As the result of full symmetry in the vertical plane view of this experiment around two perpendicular axes (X-axis and Y-axisas shown in Fig 6), one quarter of the experimental model was analytically simulated to optimize the whole number of finite elements and to reduce the computational time, as shown in Fig 6. The friction between the hangers and the soil box with sandy soil was neglected in the simulation model. The set of two rectangular plates and I-beam was simulated by stiff rectangular plates, as shown in Fig 6. The initial stiffness of the soil was assumed to be 6 MPa as the result of low initial compaction and the small thickness of the soil layer.
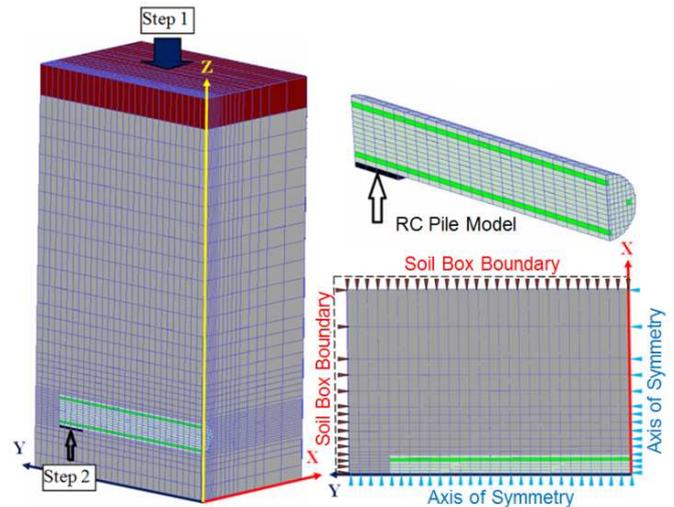

Fig. 6 Analytical model of RC pile test

The same loading procedure used in the experiment was applied on the analytical model. The first loading step was the vertical downward loading (confining load level, 10KN, 20KN, and 40KN) on the top plate as indicated in Fig 6, and then the second loading step was to upliftthe pile end to create the targeted bending tests. Joint interface elements were considered in the analytical modeling between the RC pile's outer surfaces and the surrounding soil with closure stiffnessof 10^6kgf/cm³ andshear stiffness of 500 kgf/cm³. The properties of the concrete, steel bars and Hamaoka sandy soil used in analysis are listed in Table II. Since the shear transfer model used in the program is based on the properties of reinforced concrete, the shear transfer value was reduced by roughly 25% to model the shear transfer of mortar, which was actually used in the experiment because it has fewer aggregate interlocks.

C. Analytical and Experimental Results of RC Pile Bending Test

The experimental results are fairly simulated in terms of load-displacement diagram, and the failure mode of RC pilesis focused under different levels of soil confinement. The results show that soil confinement may improve the RC pile flexural failure evolution, but the opposite effect may occur with shear failure evidence. As shown in Figs 7a, 7b, and 7c, the analytical result of the uplift load displacement curve indicates good agreement with of the experimental result for the two hangers under different levels of soil confinement magnitude. Fig 7c shows the increase in the uplift force due to the increase in the soil confinement magnitude.
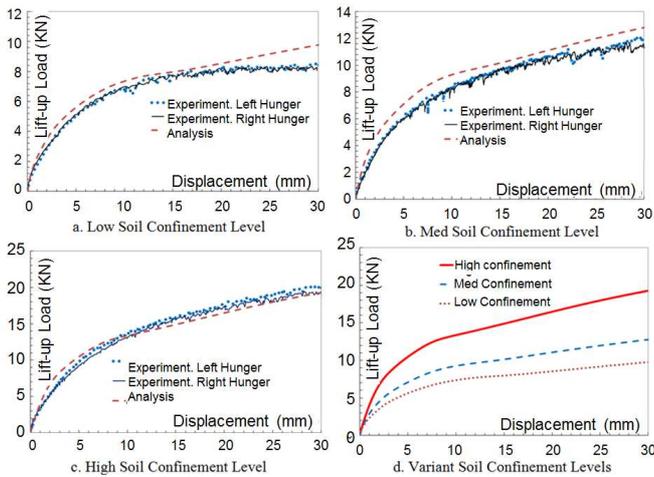
Fig. 7 Analytical and experimental uplift load-displacement of RC pile bending test

Soil confinement is expected to improve the RCpiles ductility due to reduced spalling of the concrete coverand minimized local buckling of the longitudinal steel bars in compression. Flexural failure was observed in the case of low soil confinement (Fig 8), while the dropped concrete cover was less than 3 cm long in the longitudinal direction. Local buckling of compressed steel bars was not clearly shown. Even though soil confinement may reduce the flexural failure evolution, it also may increase shear failure potential due to the high confining pressure, which may reduce the RC pile'sshear span length[12] , as illustrated by both experiments and analyses in Fig 8 (middle and high confinement cases). Both the experiment and the analysis proved that the higher the soil confinement level, the closer the concentration of flexural cracks toward the pile end. The different modes of failure (flexure, flexure-shear and shear) under soil confinement were reasonably created.
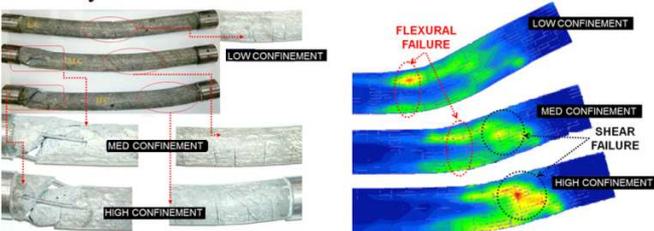

Fig. 8 Experimental and analytical damage mechanism of RC piles

IV. VERTICAL LOADING TEST FOR RC TUNNEL

This experiment was carried out in order to investigate the damage evolution of undergroundRC tunnel and/or culvert sections in an externally compressed soil foundation, and to verify the accuracy of the nonlinear analysis of static loading in view of the vertical bearing capacity. Three similar shaped small-scale models of underground ducts were made with the dimensions as shown in Fig 9. After casting concrete in the specimen forms, they were cured in wet conditions for about 120 days and then loading was carried out. The reinforcement ratio of the slab for each specimen was 0.35% using D3 deformed bars, which were developed for small-scale mockups. The concrete and steel bar properties are listed in Table 5.
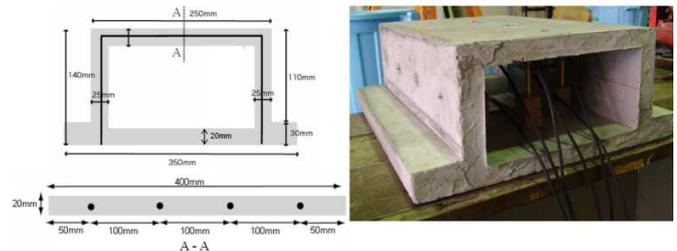

Fig. 9 RC tunnel dimensions and bar arrangement

TABLE V
MATERIAL PROPERTIES USED IN ANALYSIS OF RC TUNNEL

Soil		Reinforced Concrete	
Poisson ratio	0.20	Compressive strength	24 MPa
Dry unit weight	16 kN/m³	Unit weight	25 kN/m3
Friction angle	35 °	Tensile strength	1.5 MPa
Relative density	55 %	Steel Young modulus	2.1 x105 MPa
D50	0.2 mm	Steel yield stress	310 MPa

A. Experimental Setup of RC Tunnel Test

Before the loading experiment on soil-RC composites, the bottom of the soil box was first filled with Hamaoka sand to a depth of 5 cm (Table 4),followed by burying of the small-scale RC duct model in the same sand, as shown in Fig 10. The soil was poured and compacted by tamping in several layers to achieve a relative density of about 55%. The buried depth of the duct (D) was chosen to be 14, 28 and 42 cm in three different experiments in order to investigate its effect on the mechanistic performance of underground structures. The side walls of the soil box were lubricated to minimize the friction between the soil and the soil box. Finally, displacement- control loading was applied at the free surface of the sandy soil as shown in Fig10. The deflections of the model were measured by using pulse coders with a very high precision of 0.008 mm. Then, these pulse coders were placed inside the duct as shown in Fig 10 to measure the deflection of its different parts and obtain the load-deflection of the duct.
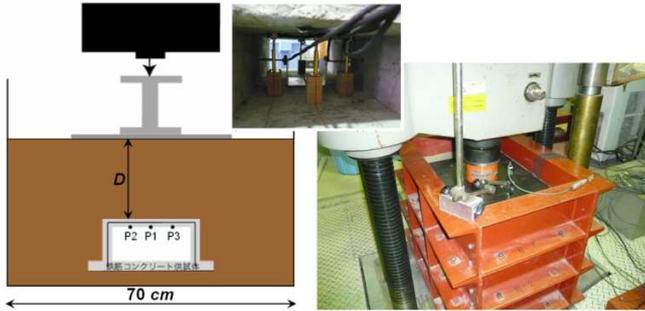
Fig. 10 RC tunnel test setup

The displacement of the loading plate was also measured by means of ordinary transducers to have a clear image of the soil surface displacement. A plate measuring 50 x 40 x 0.9 cm was selected as the loading plate. It was placed on the rather smooth surface of the soil, following the symmetry of the model with respect to the loading jack and the duct position, as shown in Fig 10.

Loading was performed in a cyclic manner and the first cycle, which caused large deformations in the soil, was carried out to compact the upper layers. Additionalloading cycles were carried out at certain levels to obtain an appropriate view of the model behavior. Loading was stopped when the deflections of the model were going to exceed the measurable range of the transducers.

B. Analytical Model of RC Tunnel

These experiments were simulated by using COM3D as described in Section 3. The properties which were considered for soil and reinforced concrete are listed in Table 5. The soil medium is divided into 4 layers by height as shown in Fig 11.
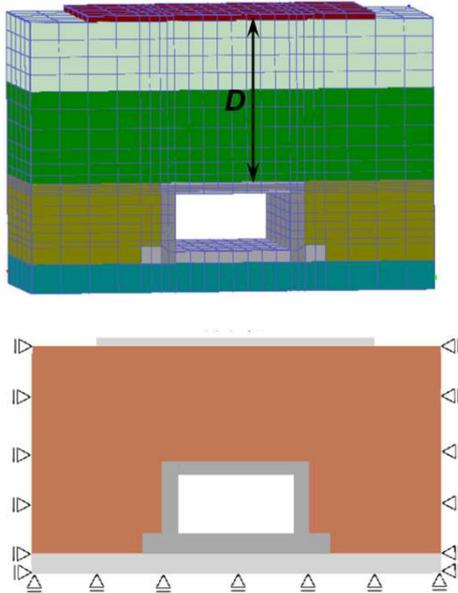

Fig. 11 Analytical model of RC tunnel test

C. Analytical and Experimental Results of Vertical Loading Test of RC Tunnel

Figure 12 compares the load-deflection curve obtained experimentally at the middle of the top slab for three different

buried depths. The simulation results for the deflection of the top slab are illustrated in Fig 13, which shows good agreement with the experimental data. The displacement of the loading plate vs. external load is compared in Fig 14 for all three experiments. Since both the reinforced concrete and soil models involved in this study are nonlinear, the good agreement between the analysis results and experimental data confirms their accuracy.

Furthermore, the cracking pattern of the specimen after the experiment, demonstrated in Fig 15, clearly implies the flexural mode of the top slab due to the external loading. This is also captured well in the analysis, where the compaction of soil layers directly affects duct nonlinearity as shown in Fig 16. In addition, the failure wedges created under the loading plate can be seen to effectively compact the sand layers and make them stiffer in the next cycle of loading. The numerical simulations prove that underground structures can carry large amount of surface loads before failure.
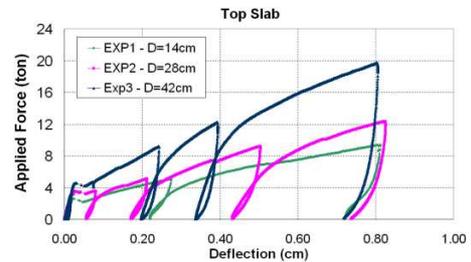

Fig. 12 Load-deflection curve at the middle of top slab
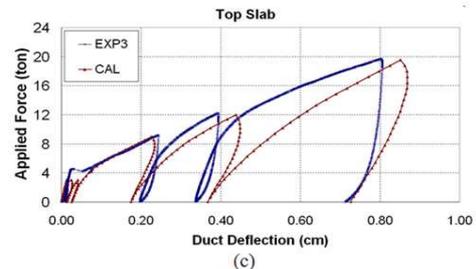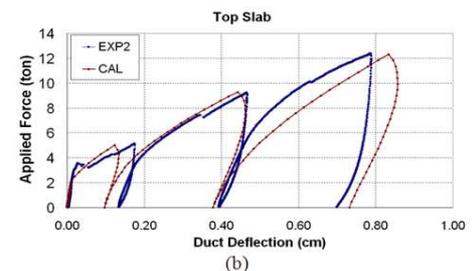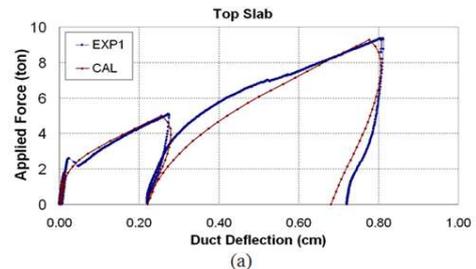

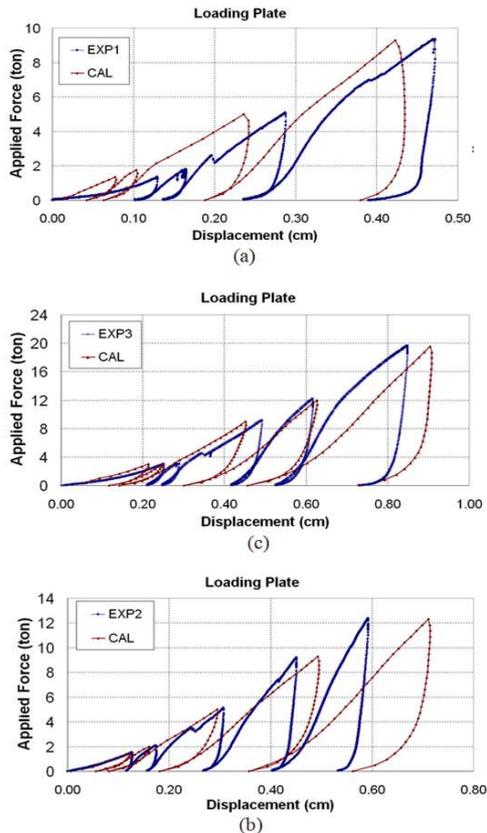Fig. 13 Deflection of top slab for different buried depths (a) D = 14 cm (b) D = 28 cm (c) D = 42 cm

Fig. 14 Displacement of loading plate for different buried depths (a) D = 14 cm (b) D = 28 cm (c) D = 42 cm

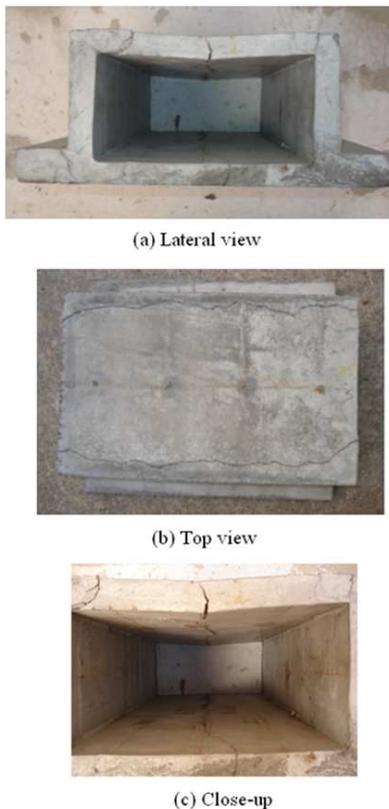(a) Lateral view

(b) Top view

(c) Close-up

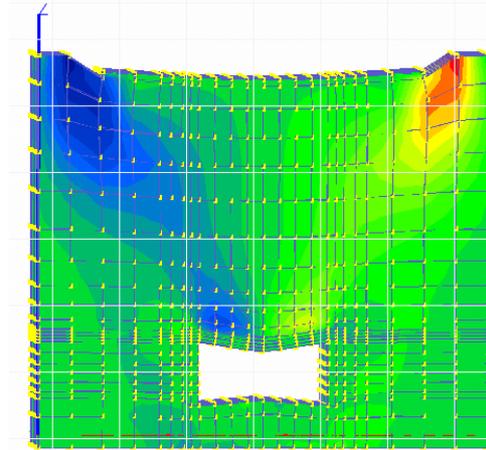Fig. 15 Crack patterns of the RC tunnel specimen after loading in experiment

Fig. 16 Shear strain profile and deflection (magnified 3 times) of the model at maximum load (D = 42 cm)

V. CONCLUSION

1) Small-scale mockups of RC piles were presented for pile-structure interaction tests, and it was demonstrated that shear failure can be successfully reproduced in experiments using small-scale pile replicas made of mortar and featuring specially manufactured deformed reinforcing bars of small sizes. In other words, the size effect of shear capacity can be traded off with the reduced shear transfer of mortar compared to normal concrete.

2) The effects of soil confinement on the RCpile modes of failure were experimentally investigated and analytically validated. Higher interacted confinement by soil may increase flexural ductility of RC piles inside the soil, but the risk of shear failure is found to rise due to the shortened shear span of the pile caused by higher confinement by soil.

3) The RC tunnel or culvertmockup of box sections and the nonlinear failure simulation revealed that the soil foundation including the underground tunneland/or culvert may maintain vertical bearing capacity even though flexural failure of RC tunnel slabs takes place due to the stress redistribution of soil caused by the reduction of structural stiffness of the tunnel boxes. This means in practice that the ultimate limit state of RC underground members does not necessarily coincide with the ultimate capacity of soil-RC interacting systems.

4) Behavioral simulation was applied to the soil-pile and soil-tunnel interaction problems as described above and nonlinear stiffness changes in structures and associated re-distributions of stress in soil were reasonably simulated. The trade-off of the size effect of RC shear with the reduced shear transfer along cracks was quantitatively verified by considering both tension softening of concrete and the reduced shear transfer of mortar without coarse aggregates.

REFERENCES

[1] Hamada, M.(1992). "Large ground deformations and their effects on lifelines: 1964Niigata earthquake. Case studies of liquefaction and lifelines performance during past earthquakes," Technical Report NCEER-92-0001, Volume 1, Japanese Case Studies, National Centre for Earthquake Engineering Research. Buffalo, NY.

[2] EERI (2010). "The Mw 7.0 Haiti Earthquake of January 12, 2010," Report 1, Special Earthquake Report, Earthquake Engineering Research Institute.

[3] Wilson, D. W. (1998) "Soil-pile-superstructure interaction in liquefying sand and soft clay," PhD thesis, University of California, Davis, CA.

[4] Towhata, I. (2008). "Geotechnical Earthquake Engineering," Springer, Germany.

[5] Maekawa, K., Pimanmas, A. and Okamura, H. (2003). "Nonlinear Mechanics of Reinforced Concrete," Spon Press, London.

[6] Maki, T., Maekawa, K., and Mutsuyoshi, H. (2005). "RC pile-soil interaction analysis using a 3D-finite element method with fiber theory-based beam elements," Earthquake Engineering and Structural Dynamics, 99, 1-26.

[7] Tuladhar, R., Maki, T., and Mutsuyoshi, H. (2008). "Cyclic behavior of laterally loaded concrete piles embedded into cohesive soil," Earthquake Engineering and Structural Dynamics, 37, 43–59.

[8] Okhovat, M. R., and Maekawa, K.(2009) " Damage control of underground RC structures subjected to service and seismic loads," PhD thesis, University of Tokyo.

[9] Kato, B. (1979). "Mechanical properties of steel under load cycles idealizing seismic action," CEB Bulletin D'Information, 131, 7-27.

[10] Towhata, I. and Ishihara, K. (1985) "Modeling soil behaviors under principal stress axes rotation," 5th Int. Conf. on Numerical Method in Geomechanics, Nagoya, 523-30.

[11] Masing, G.(1926)"Eigenspannungen and VerfestigungBeim Messing," Proc. of Second International Congress of Applied Mechanics, 332, Zurich.

[12] Konagai, K., Yin, Y., and Murono, Y. (2003) "Single beam analogy for describing soil–pile group interaction," Soil Dynamics and Earthquake Engineering, 23, 213-221.

[13] Maekawa, K. and An, X. (2000). "Shear failure and ductility of RC columns after yielding of main reinforcement," Engineering Fracture Mechanics, 65, 335-368.

[14] Li, B., Maekawa, K. and Okamura, H. (1989). "Contact density model for stress transfer across crack in concrete," Journal of Faculty of Engineering, University of Tokyo (B), 40(1), 9-52.

[15] Nam, S. H., Songa, H. W., Byuna, K. J., Maekawa, K. (2006)" Seismic analysis of undergroundreinforced concrete structures consideringelasto-plastic interface element with thickness,"Engineering Structures, 28, 1122-1131.